Journal of Power Sources 196 (2011) 1084–1089

Contents lists available at ScienceDirect

Journal of Power Sources

journal homepage: www.elsevier.com/locate/jpowsour

An investigation of Pt alloy oxygen reduction catalysts in phosphoric acid doped PBI fuel cells

M. Mamlouk, K. Scott*

School of Chemical Engineering and Advanced Materials, Merz Court, Newcastle University, Newcastle upon Tyne, NE17RU, UK

ARTICLE INFO

Article history:
Received 18 September 2009
Received in revised form 9 August 2010
Accepted 10 August 2010
Available online 17 August 2010

Keywords:
Phosphoric acid
Polybenzimidazole
Fuel cell
Oxygen reduction
Pt alloy catalysts
Electrode performance

ABSTRACT

A study of a phosphoric acid doped polybenzimidazole (PBI) membrane fuel cell using commercial carbon supported, Pt alloy oxygen reduction catalysts is reported. The cathodes were made from PTFE bonded carbon supported Pt alloys without PBI but with phopshoric acid added to the electrode for ionic conductivity. Polarisation data for fuel cells with cathodes made with alloys of Pt with Ni, Co, Ru and Fe are compared with those with Pt alone as cathode at temperatures between 120 and 175 °C. With the same loading of Pt enhancement in cell performance was achieved with all alloys except Pt–Ru, in the low current density activation kinetics region of operation. The extent of enhancement depended upon the operating temperature and also the catalyst loading. In particular a Pt–Co alloy produced performance significantly better than Pt alone, e.g. a peak power, with low pressure air, of 0.25 W cm^{-2} with 0.2 mg Pt cm^{-2} of a 20 wt% Pt–Co catalyst.

1. Introduction

Following on from the success of the phosphoric acid fuel cell and the low temperature polymer electrolyte fuel cell (PEMFC) there has been significant interest in intermediate temperature operation PEMFCs in recent years [1–3]. In particular cell technology based on phosphoric acid doped polybenzimidazole (PBI) membranes has been actively developed [4–18] and started to approach commercialisation. Recent studies of PBI based fuel cells which have considered the effect of the catalytic ink preparation method [12]; preparation and operation of gas diffusion electrodes [13]; influence of catalyst layer binder on catalyst utilization [14]; acid migration in phosphoric acid doped polybenzimidazole (PBI) membrane [15].

Due to the similar operating environment of electrodes in PAFCs and PBI based cells much of the research on the former is relevant to that of the latter regarding catalytic activity and the influence of phosphoric acid.

Oxygen reduction activity of various platinum alloys has been reported for phosphoric acid electrolytes [19–28]. Oxygen reduction activity in hot phosphoric acid (200 °C) on platinum and platinum alloys increased linearly as the nearest-neighbour distance in the electrocatalyst decreased. A composite analysis shows that data for supported platinum alloys [20] were consistent with bulk metal data [19] with respect to specific activity, activation energy, pre-exponential factor and percent d-band character. The kinetic parameters of the oxygen reduction reaction, in hot concentrated phosphoric acid, on highly dispersed platinum have been rationalized in terms of the rate determining step being the rupture of the O–O bond via various dual site mechanisms [21].

In phosphoric acid the (Pt–M/C) alloyed, disordered structure interact more strongly with impurities than the ordered structures (Pt/C). Chromium addition caused a decrease in Tafel slope due to oxide reduction effects [22]. It was found that the Tafel slope measured at room temperature and atmospheric pressure on platinum increased from −110 mV dec^{-1} in low H_3PO_4 concentrations (10 wt%) to −134 mV dec^{-1} in 85 wt% H_3PO_4. Whilst the Tafel slopes for Pt–Co (90:10 a/o) and Pt–Cr (65:35 a/o) changed from 111 and 101, at low concentration, to 126 and 118 mV dec^{-1} with 85 wt% H_3PO_4, respectively [23]. Anodic adsorption isotherms indicated that the high H_3PO_4 concentrations also obstructed adsorption of oxygen from solution [23].

Appleby [24] studied oxygen reduction on various metals and alloys in phosphoric acid. For Pt–Ru alloys it was concluded that i_0 for ORR decreased and Tafel slope increased by increasing the ruthenium content in the alloy. Similarly, the activation energy for ORR in H_3PO_4 fell when moving from pure platinum (22.9 kcal mol^{-1}) to pure ruthenium (11.7 kcal mol^{-1}). This means that at elevated temperatures the platinum exchange current den-

* Corresponding author. Tel.: +44 1912228771; fax: +44 1912225292.
E-mail address: k.scott@ncl.ac.uk (K. Scott).

0378-7753/$ – see front matter © 2010 Elsevier B.V. All rights reserved.
doi:10.1016/j.jpowsour.2010.08.021

sity will overtake that of pure ruthenium at ~80°C and Pt–Ru (1:1) at ~100 °C.

Pt–Fe (75:25 a/o) catalysts were also studied for oxygen reduction in PAFC. The mass activity (mA g^{-1} Pt) of the alloyed catalyst was about the same as that of the pure Pt catalyst due to the particle sintering in the alloyed catalyst. However, the specific activity (mA m^{-2} Pt, based on UPD) of the alloyed catalyst was twice that of pure Pt catalyst [25].

On the contrary, Pt–Co activity tests under phosphoric acid fuel cell conditions demonstrated that the most highly alloyed catalysts were not significantly more active than pure Pt catalyst of comparable crystallite size [26]. Loss of cobalt in the phosphoric acid environment was the lowest in catalysts which were the most alloyed, and where the Pt–Co (3:1) ordered phase was present [26]. It was found that the clean annealed surface of the alloy was pure Pt and the subsurface is enriched in Co [27]. Furthermore, this Pt surface did not behave like pure Pt for the chemisorption of carbon monoxide or oxygen [28]. The alloyed Pt-surface binds CO less strongly and oxygen more strongly. However, when heated in oxygen at fuel cell temperatures, even at very low pressures, the surface region is de-alloyed by oxidation to form a cobalt oxide over-layer [28]. The oxide over-layer dissolved in hot concentrated phosphoric acid, leaving a de-alloyed pure Pt surface region on top of the bulk alloy.

Overall there have been significant studies of Pt alloys in PAFC cell similar cell conditions but no evaluation of such electrocatalysts and cathodes in PA doped PBI membrane fuel cells. This paper reports data obtained for the cell performance of PBI based fuel cells using a range of Pt alloy ORR electrocatalysts. The performance data is generally in agreement with data obtained on ORR electrocatalysts in concentrated phosphoric acid [17].

2. Experimental

2.1.1. Cell design

The fuel cell used in experiments was made from titanium and is shown schematically in Fig. 1. The cell body had a 3 cm × 3 cm gold plated parallel flow fields. Mica filled PTFE inserts were used to surround the flow fields and provide location for the O-ring seal and a dynamic hydrogen electrode (DHE). The solid state DHE consisted of two platinum wires on each side of the membrane located outside the O-ring: a distance of 10 mm away from the MEA edge to avoid side current effects (the membrane used was ~50 μm thick). A small current of 1.0 mA cm^{-2} (~10 μA) was applied by means of 9.0 V battery connected in series with an appropriate resistance.

The temperature of the cell was controlled by thermostatically controlled cartridge heaters inserted into the cell body. The gases were passed into a home-made humidifier at 16 °C prior to entering the cell at ambient temperature; this provided small humidification of 0.36% RH at 150 °C (unless otherwise mentioned). The flow rates were controlled manually by means of appropriate flow meters designated for each gas (Platon, RM&C, U.K.). The cell was tested under ambient pressure unless otherwise specified.

2.1.2. Instruments

A 20A potentiostat (Powerstat, Sycopel, U.K.) combined with a high impedance multi-channel data acquisition card (national instrument, NI6010) was used to carry out the electrochemical measurements, which enabled continuous monitoring of anode, cathode (vs. DHE) and cell performances separately.

The conductivity of MEAs was measured using a Gill AC frequency response analyzer (ACM instruments, U.K.) and the relative humidity was obtained from an intrinsically safe humidity sensor (Vaisala HUMICAP®, Finland).

2.1.3. Electrode preparation

A spraying machine was used to deposit catalyst layers; to achieve a reproducible spraying pattern and catalyst layer structure/porosity. A CNC milling machine (Sherline 2010, USA) was used to provide the desired spraying pattern, whilst a fixed stainless steel spraying (0.5 mm) nozzle (Schlick 970S8, Germany) and associated metering valve was used to control the spray mixture (with nitrogen) and ink flow rate.

The catalyst ink was prepared by sonicating the catalyst and PTFE dispersion (60 wt%, Aldrich) in a water–ethanol mixture, for PTFE based MEAs. The required amount of PA acid was then added to the surface by means of a micro-pipette and the electrodes were left for a week to obtain uniform acid distribution.

Gas diffusion electrodes (carbon cloth) incorporated with wet proofed micro-porous layer (H2315 T10AC1) obtained from Freudenberg (FFCCT, Germany) were used as substrates to deposit the catalyst layer for both anode and cathode.

Four different Pt alloys obtained from Etek, USA were studied:

1. 30% Pt–Fe/C, which contained 20% Pt.
2. 60%Pt–Ru/C, which contained 40% Pt.
3. 20%Pt–Ni/C and 20%Pt–Co/C, which contained 17% Pt.

Comparisons are made with Pt catalysts of similar %wt i.e. 20%, 30% and 40% Pt.

The MEA was obtained by hot pressing the electrodes on 5.6 mol% phosphoric acid doped PBI membrane at 150 °C for 10 min with a load of 40 kg cm^{-2}. Note that each PBI unit can hold two acid molecules by hydrogen bonding to the two imidazole rings. After the maximum protonation of the nitrogen atoms is reached (at 2 PRU), any further acid will be free mobile acid, held in the membrane matrix

3. Results and discussion

While PBI is considered a good candidate for membrane materials due to its low permeability, addition of PBI to the catalyst layer as ionomer for proton conduction through the catalyst layer and binder, can impose mass transport limitation on anode and cathode performance depending on the thickness of the film formed on the catalyst sites. Furthermore, addition of phosphoric acid is necessarily to facilitate oxygen permeability and proton conduction, as the conductivity of non-doped PBI is very low (in the range of 10^{-4} S cm^{-1}).

In this study, we eliminated PBI from the catalyst structure and relied on the conductivity of phosphoric acid as electrolyte, to give the following advantages:

- Conductivity of phosphoric acid 0.568 S cm^{-1} at 150 °C is an order of magnitude higher than that of doped PBI 6 PRU ~0.047 S cm^{-1} at 150 °C and 5% RH.
- Oxygen diffusion in phosphoric acid (98 wt%) 30×10^{-6} cm^2 s^{-1} is an order of magnitude higher than that of doped PBI 6 PRU 3.2×10^{-6} cm^2 s^{-1} at 150 °C.
- Dissolved oxygen concentrations (solubility), 0.68×10^{-6} mol cm^{-3} for doped PBI 6 PRU compared to 0.5×10^{-6} mol cm^{-3} for 95 wt% phosphoric acid at 150 °C and atmospheric pressure.

PTFE was introduced in the catalyst layer to act as binder, to provide an amorphous phase to hold the phosphoric acid,

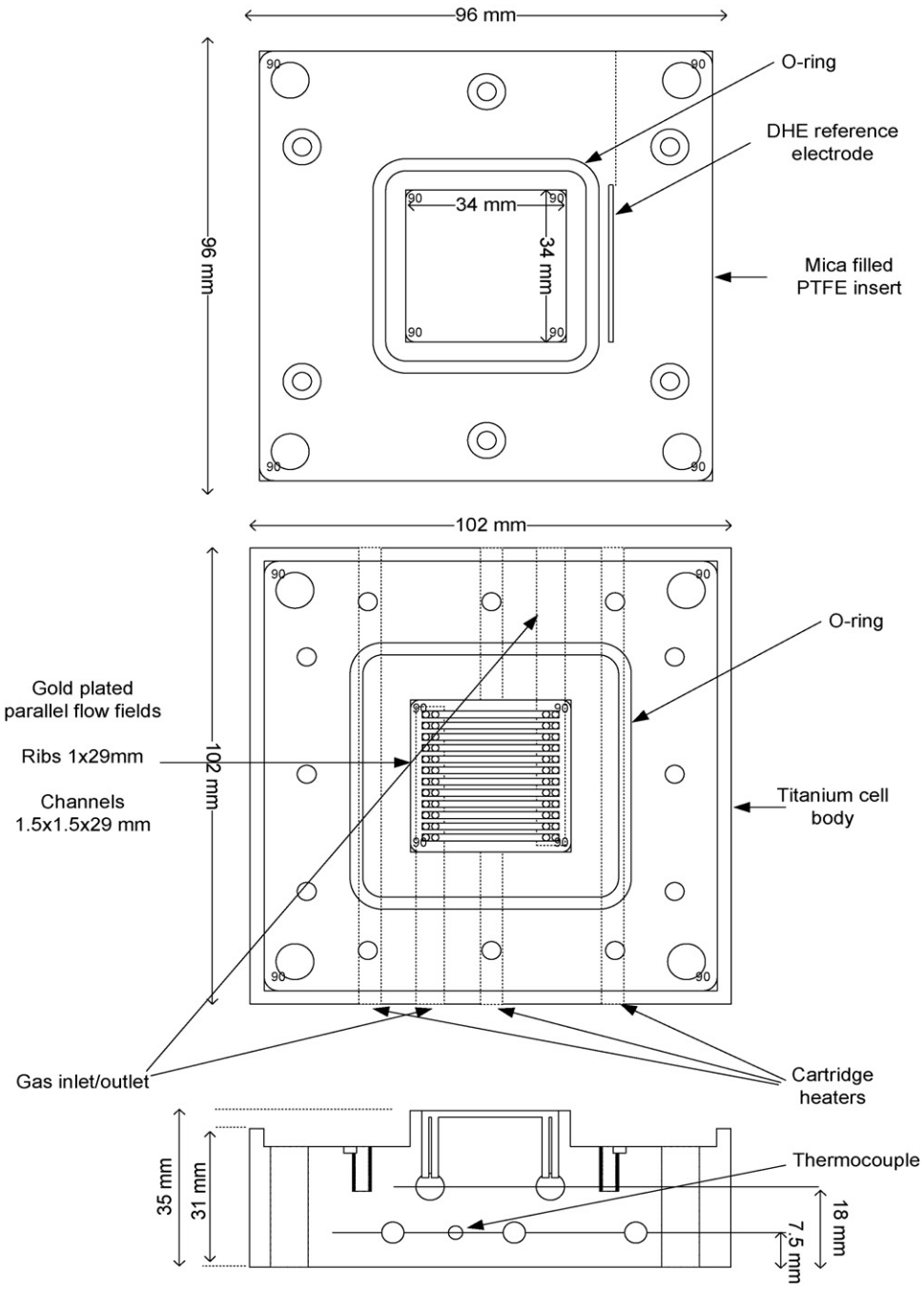

Fig. 1. Schematic diagram of the titanium fuel cell.

enhance porosity and to facilitate transport of oxygen to the catalyst layer by repelling the phosphoric acid from the catalyst structure (hydrophobic properties) and provide higher oxygen permeability (two order of magnitude), e.g. at 80 °C PTFE exhibits an oxygen permeability of 6.1 mol cm cm^{-2} s^{-1} atm^{-1} compared to 0.05 mol cm cm^{-2} s^{-1} atm^{-1} for pristine PBI [4].

Four different Pt alloys were studied in this work; 30% Pt–Fe/C, 60%Pt–Ru/C, 20%Pt–Ni/C and 20%Pt–Co/C (Etek, USA). All the studied alloys had atomic ratios of (1:1 a/o) whilst the average particles size (from XRD) was in the range of 3–4 nm except for Pt–Ru alloys which was in the range of 2–3 nm. Their performance was compared to that of pure Pt/C with similar platinum weight percentages, i.e. 20%, 30% and 40% Pt/C, with average particles size (XRD) of 2.2, 2.5 and 2.8 nm, respectively. The platinum loading was 0.4 mg Pt cm^{-2} for Pt–Fe and Pt–Ru, whilst a loading of 0.2 mg Pt cm^{-2} was used for Pt–Ni and Pt–Co, due to the low metal to carbon ratio, to try and maintain a desired catalyst layer thickness to minimize mass transport effects on the cell polarisation.

Fig. 2 compares cell performance under with various oxygen concentrations at 150 °C for MEAs using 40% Pt–Fe/C (~30% Pt) and 30% Pt/C cathode electrodes utilising 0.4 mg Pt cm^{-2} with 40 wt% PTFE. Open circuit potentials with both cathodes were around 0.9 V. The Pt–Fe alloy showed clear advantages in the kinetic region (low current densities) over standard platinum, with some 20–30 mV higher potentials, at all the studied oxygen concentrations. The observed kinetic enhancement was not due to the catalyst layer structure, as both electrodes had similar Pt:C ratios (30 wt%) and loading of 0.4 mg Pt cm^{-2}. The data confirm the reported advan-

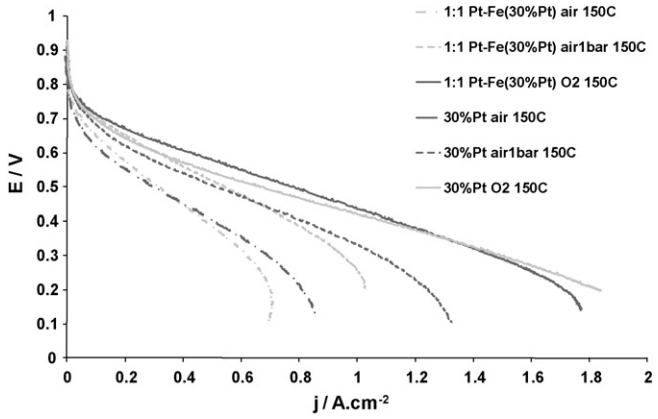

Fig. 2. Compares cell performance under various oxygen concentrations at 150 °C of MEAs using 40% Pt–Fe/C (~30% Pt) and 30% Pt/C cathode electrodes utilising 0.4 mg Pt cm^{-2} with 40 wt% PTFE.

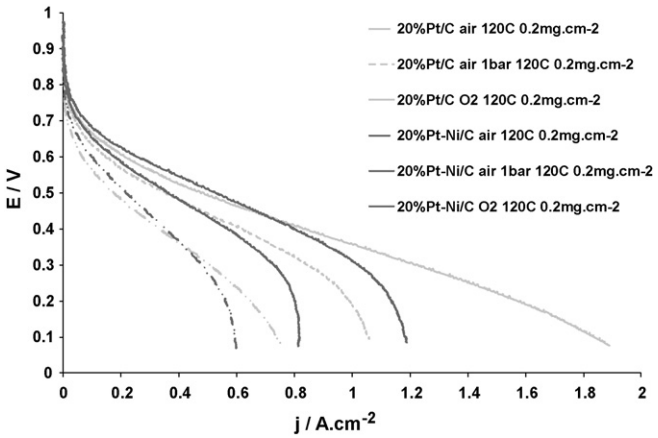

Fig. 4. Compares cell performance under various oxygen concentrations at 120 °C of MEAs using 20% Pt–Ni/C (~17% Pt) and 20% Pt/C cathode electrodes utilising 0.2 mg Pt cm^{-2} with 40 wt% PTFE.

tage of Pt alloying (with iron) for ORR kinetics [25]. The Pt–Fe alloy cathode exhibited somewhat lower limiting current densities than Pt alone which may be a result of a slightly thicker catalyst layer for the former material.

Fig. 3 compares cell performance under various oxygen concentrations at 150 °C for MEAs using 60% Pt–Ru/C (~40% Pt) and 40% Pt/C cathodes utilising 0.4 mg Pt cm^{-2} with 40 wt% PTFE. Open circuit potentials were noticeably lower with the Pt–Ru alloy cathode particular at low oxygen partial pressure. From the data it can be seen that with Pt–Ru cathodes, current densities were much lower (at a given potential) than with Pt. There were large potential losses in the polarisation curves, without an apparent linear region or limiting current; suggesting that the electrode was mainly under pure activation control due to the slow kinetics of oxygen reduction in Pt–Ru alloy electrocatalyst surface as has been reported previously [24]. Thus Pt–Ru alloy is not a suitable catalyst for oxygen reduction due to the large overvoltage losses encountered in the kinetic region.

Fig. 4 compares cell performance under various oxygen concentrations at 120 °C of MEAs using 20% Pt–Ni/C (~17% Pt) and 20% Pt/C cathode electrodes utilising 0.2 mg Pt cm^{-2} with 40 wt% PTFE. Figs. 5 and 6 compare the alloy performance (0.2 mg Pt cm^{-2}) with 0.4 mg Pt cm^{-2} for 30% Pt/C at temperatures of 120 and 175 °C, respectively. All data show the expected improvement in cell performance on increasing the oxygen partial pressure.

It can be seen from Fig. 4 that the Pt–Ni alloy produced slightly higher potentials (enhanced kinetics for the ORR), at lower current densities, when compared to standard platinum (20%Pt/C, same loading) at 120 °C, even though the alloy had a smaller electrochemical surface area, as a result of alloying (average particles size of 3–4 nm) in comparison to the standard platinum (2.2 nm). Thus in a practical fuel cell potential operating range the Pt–Ni alloy would offer higher fuel efficiencies and power densities.

Additionally, the Pt–Ni alloy at loading of 0.2 mg Pt cm^{-2} gave similar cell voltage characteristics in the kinetic region (up to a typical operating voltage of 0.6 V) to that of 30% Pt/C with a loading of 0.4 mg Pt cm^{-2}. However, any enhancement in performance disappeared at elevated temperatures. At 150 °C (data not shown) the Pt–Ni alloy showed a similar performance to that of platinum (20%Pt/C, 0.2 mg Pt cm^{-2}) and at 175 °C the 0.2 mg Pt cm^{-2} Pt–Ni/C alloy gave inferior performance to that of 30% Pt/C with a loading of 0.4 mg Pt cm^{-2} (Fig. 5) over the entire potential range.

It was also observed that the limiting current densities for the cell with the Pt–Ni alloy were much lower than with the Pt catalysts. Incorporation of Ni and the resultant higher particle size and lower porosity would appear to have caused greater mass transport limitations due potentially to thicker films of PA over the electrocatalyst.

Fig. 7 compares cell performance under various oxygen concentrations at 150 °C for MEAs using 20% Pt–Co/C (~17% Pt) and 20% Pt/C cathodes utilising 0.2 mg Pt cm^{-2} with 40 wt% PTFE. The

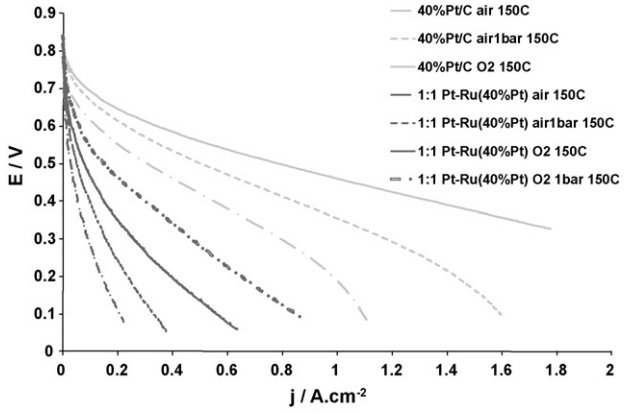

Fig. 3. Compares cell performance under various oxygen concentrations at 150 °C of MEAs using 60% Pt–Ru/C (~40% Pt) and 40% Pt/C cathode electrodes utilising 0.4 mg Pt cm^{-2} with 40 wt% PTFE.

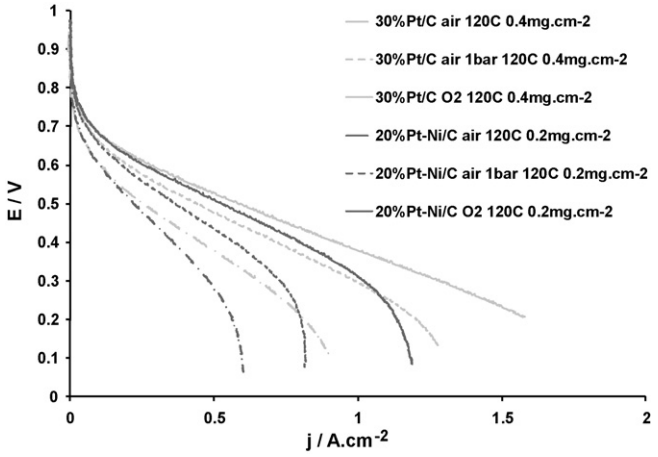

Fig. 5. Compares cell performance under various oxygen concentrations at 120 °C of MEAs using 20% Pt–Ni/C (~17% Pt) and 30% Pt/C cathode electrodes utilising 0.2 mg Pt cm^{-2} for the alloy and 0.4 mg Pt cm^{-2} for pure Pt with 40 wt% PTFE.

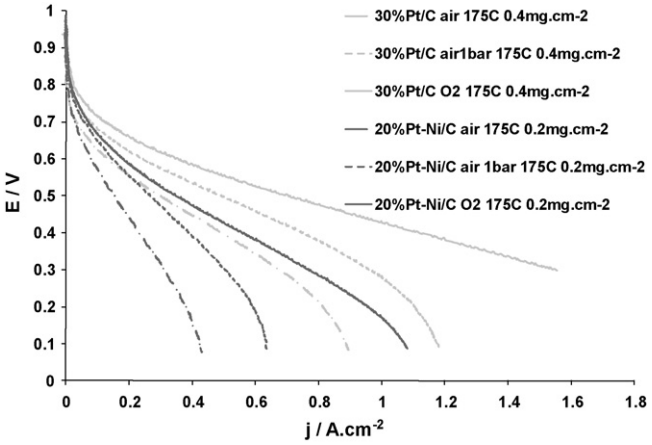

Fig. 6. Compares cell performance under various oxygen concentrations at 175 °C of MEAs using 20% Pt–Ni/C (~17% Pt) and 30% Pt/C cathode electrodes utilising 0.2 mg Pt cm^{-2} for the alloy and 0.4 mg Pt cm^{-2} for pure Pt with 40 wt% PTFE.

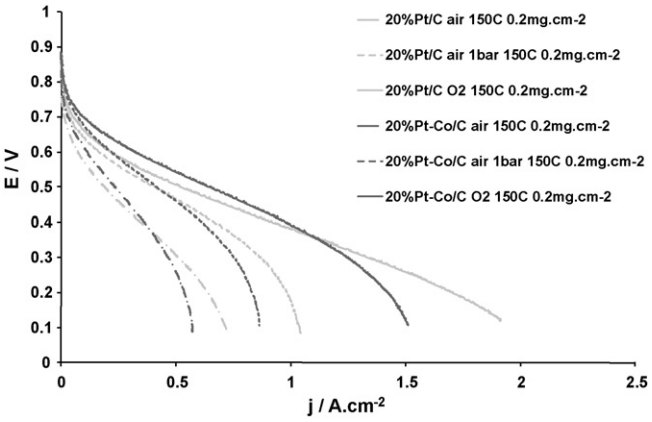

Fig. 7. Compares cell performance under various oxygen concentrations at 150 °C of MEAs using 20% Pt–Co/C (~17% Pt) and 20% Pt/C cathode electrodes utilising 0.2 mg Pt cm^{-2} with 40 wt% PTFE.

Pt–Co alloy performance was similar to that of the Pt–Ni alloy, i.e. it showed higher potentials than achieved with the standard 20% Pt/C at 120 °C (both with loading of 0.2 mg Pt cm^{-2}) even though

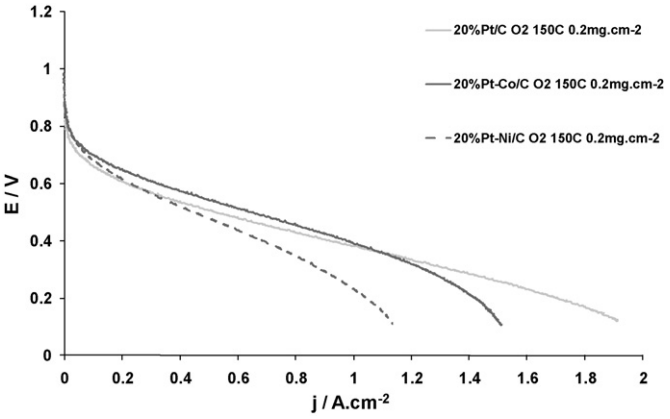

Fig. 8. Comparison of cell performance of Pt–Co, Pt–Ni and Pt at 150 °C.

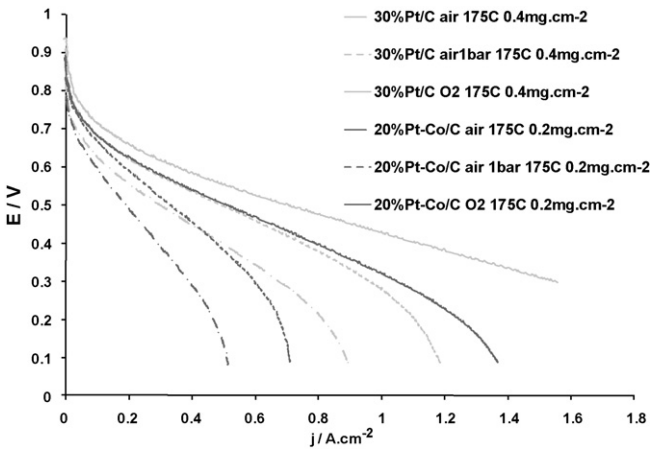

Fig. 9. Compares cell performance under various oxygen concentrations at 175 °C of MEAs using 20% Pt–Co/C (~17% Pt) and 30% Pt/C cathode electrodes utilising 0.2 mg Pt cm^{-2} for the alloy and 0.4 mg Pt cm^{-2} for pure Pt with 40 wt% PTFE.

that the alloy had a smaller ESA. The Pt–Co alloy maintained its better performance (unlike Pt–Ni) than Pt (20%Pt/C, 0.2 mg Pt cm^{-2}) at a temperature of 150 °C (Fig. 8).

Fig. 9 shows cell performance under various oxygen concentrations at 175 °C of MEAs using 20% Pt–Co/C (~17% Pt) and 30%

Table 1A
Maximum power densities and current densities at 0.6 V for MEAs utilising Pt and Pt–M alloys at 120 °C.

	Power density air (1 bar) (W cm^{-2})	Power density O_2 (atm) (W cm^{-2})	j at 0.6 V air (1 bar) (A cm^{-2})	j at 0.6V O_2 (atm) (A cm^{-2})
0.4 mg cm^{-2} 30%Pt/C	0.304	0.568	0.205	0.28
0.2 mg cm^{-2} 20%Pt/C	0.262	0.371	0.145	0.215
0.2 mg cm^{-2} 20%Pt–Ni/C	0.231	0.328	0.18	0.26
0.2 mg cm^{-2} 20%Pt–Co/C	0.256	0.374	0.18	0.235
0.4 mg cm^{-2} 30%Pt–Fe/C	0.256	0.434	0.25	0.35

Table 1B
Maximum power densities and current densities at 0.6 V for MEAs utilising Pt and Pt–M alloys at 150 °C.

	Power density air (1 bar) (W cm^{-2})	Power density O_2 (atm) (W cm^{-2})	j at 0.6V air (1 bar) (A cm^{-2})	j at 0.6V O_2 (atm) (A cm^{-2})
0.4 mg cm^{-2} 30%Pt/C	0.339	0.486	0.255	0.31
0.2 mg cm^{-2} 20%Pt/C	0.277	0.406	0.163	0.215
0.2 mg cm^{-2} 20%Pt–Ni/C	0.196	0.28	0.18	0.225
0.2 mg cm^{-2} 20%Pt–Co/C	0.249	0.404	0.215	0.32
0.4 mg cm^{-2} 30%Pt–Fe/C	0.313	0.468	0.31	0.44

Pt/C cathode electrodes utilising 0.2 mg Pt cm^{-2} for the alloy and 0.4 mg Pt cm^{-2} for pure Pt with 40 wt% PTFE. It is clear that at 175 °C the 0.2 mg Pt cm^{-2} Pt–Co alloy had an inferior performance compared to 0.4 mg Pt cm^{-2} 30% Pt/C, whilst at 150 °C both electrodes showed comparable performance in the kinetic region of the polarisation curves. This behaviour suggests that the alloy performance did not improve with an increase in temperature as much as did the platinum catalyst. However, it has been shown in the literature that Pt–Ni and Pt–Co alloys exhibit similar activation energies for oxygen reduction to that of platinum [26].

It has been reported that cobalt dissolution was a common problem for Pt–Co alloy in PAFCs [26]. The degradation and the dissolution process is expected to occur over hundreds hours of operation and not over the short period of experiments (3 days) used in this study. In this study it was observed that recovery in the performance (or in other words the alloys enhanced performance) over standard platinum returned when the temperature was lowered to 120 °C in case of Pt–Ni and Pt–Co. The performance of the fuel cells with the Pt alloy and Pt catalysts was reproducible and remained stable over the operation period of the fuel cells, which for each MEA was 5 days of intermittent operation, i.e. 8 h of cell testing and 16 h at open circuit per day.

This suggests that the observed effect of temperature on performance was not due to dissolution, but due to a drop in water activity at elevated temperatures, where phosphoric acid started to dehydrate [14]. The fall in water activity at elevated temperatures results in an increase in ORR activity for Pt/C due to lowering of surface oxide formation, a corresponding effect with Pt alloys does not occur.

Tables 1A and 1B summarise the performance of the fuel cell using the Pt alloys with Co, Fe and Ni and with Pt alone as cathode electrocatalysts. The data enable comparisons in performance to be made in terms of peak power density and current densities achieved at a cell voltage of 0.6 V (typically in the activation controlled region, with some Ohmic polarisation losses). The latter voltage is selected to represent a minimum voltage suitable for practical fuel cell operation. The benefits of using Pt alloys in terms of higher current densities at a fixed potential and higher maximum power densities is apparent from this data.

Overall this work has demonstrated the potential use of Pt alloys as catalyst in PA doped PBI membrane fuel cells. Although the short-term performance over days of operation was consistent, the use of Pt alloy cathode catalysts in such fuel cells requires long-term evaluation, which was outside the scope of the current work.

4. Conclusions

Intermediate temperature phosphoric acid doped PBI membrane fuel cells have been successfully operated with carbon supported Pt alloy catalyst in the cathodes, in which ionic conductivity was achieved by simple phosphoric acid doping. Alloys of Pt with Fe, Ni and Co all enhanced the fuel cell performance in the low current density (high potential) activation region. In particular Pt/Co alloy catalysts gave some 25 and 50 mV higher potentials at 0.2 A cm^{-2} with air and 0.5 A cm^{-2} with oxygen in comparison to Pt alone with oxygen and air. At low voltages, i.e. high current densities, the performance of the fuel cells with Pt alloys was lower than those with Pt alone.

Acknowledgements

The EPSRC, through the SUPERGEN Fuel cell Consortium, and the EU, through the FP6 project FURIM, supported this work.

References

[1] D.J. Jones, J. Roziere, J. Membr. Sci. 185 (1) (2001) 41–58.
[2] O. Savadogo, J. Power Sources 127 (1–2) (2004) 135–161.
[3] D.J. Jones, J. Roziere, Annu. Rev. Mater. Res. 33 (2003) 503–555.
[4] J.T. Wang, R.F. Savinell, J. Wainright, M. Litt, H. Yu, Electrochim. Acta 41 (2) (1996) 193–197.
[5] J.S. Wainright, J.T. Wang, D. Weng, R.F. Savinell, M. Litt, J. Electrochem. Soc. 142 (7) (1995) L121–L123.
[6] B.Z.O. Xing, Savadogo, J. New Mater. Electrochem. Syst. 2 (2) (1999) 95–101.
[7] Q.F. Li, R.H. He, J.A. Gao, J.O. Jensen, N.J. Bjerrum, J. Electrochem. Soc. 150 (12) (2003) A1599–A1605.
[8] Q.F. Li, R.H. He, R.W. Berg, H.A. Hjuler, N.J. Bjerrum, Solid State Ionics 168 (1–2) (2004) 177–185.
[9] S.R. Samms, S. Wasmus, R.F. Savinell, J. Electrochem. Soc. 143 (4) (1996) 1225–1232.
[10] K. Scott, M. Mamlouk, Battery Bimonthly 36 (5) (2006) p11.
[11] Q.F. Li, H.A. Hjuler, N.J. Bjerrum, J. Appl. Electrochem. 31 (7) (2001) 773–779.
[12] J. Lobato, M.A. Rodrigo, J.J. Linares, K. Scott, J. Power Sources 157 (2006) 284–292.
[13] Chao Pan Qingfeng Li, Jens Oluf Jensen, Ronghuan Heb, N. Lars, Cleemann, S. Morten, Nilsson, J. Niels, Bjerrum, Zeng. Qingxue, J. Power Sources 172 (2007) 278–286.
[14] A.D. Modestov, M.R. Tarasevich, V.Y. Filimonov, Membr. J. Electrochem. Soc. 156 (2006) B650–B656.
[15] O. Yuka, S. Atsuo, H. Michio, J. Power Sources (2009) 943–949.
[16] J. Lobato, P. Cañizares, M.A. Rodrigo, J.J. Linares, Electrochim. Acta 52 (2007) 3910–3920.
[17] M. Mamlouk, K. Scott, Fuel Cell Sci. Technol., 2010, in press.
[18] Q. Li, J.O. Jensen, R. He, G. Xiao, J.A. Gao, R.W. Berg, H.A. Hjuler, H. Hennesoe, N.J. Bjerrum, Recent Res. Dev. Electrochem. 6 (2003) 1–26.
[19] A.J. Appleby, Catal. Rev. 4 (1) (1970) 221–244.
[20] V.E.J. Jalan, Taylor, J. Electrochem. Soc. 130 (11) (1983) 2299–2302.
[21] W.M.J.M. Vogel, Baris, Electrochim. Acta 22 (11) (1977) 1259–1263.
[22] J.T. Glass, G.L. Cahen, G.E. Stoner, E.J. Taylor, J. Electrochem. Soc. 134 (1) (1987) 58–65.
[23] J.T. Glass, G.I. Cahen, G.E. Stoner, J. Electrochem. Soc. 136 (3) (1989) 656–660.
[24] A.J. Appleby, J. Electroanal. Chem. 27 (3) (1970) 347–354.
[25] K.T. Kim, J.T. Hwang, Y.G. Kim, J.S. Chung, J. Electrochem. Soc. 140 (1) (1993) 31–36.
[26] B.C.P.N. Beard, Ross, J. Electrochem. Soc. 137 (11) (1990) 3368–3374.
[27] U. Bardi, A. Atrei, P.N. Ross, E. Zanazzi, G. Rovida, Surf. Sci. 211–212 (1989) 441–447.
[28] U. Bardi, B. Beard, P. Ross, J. Vac. Sci. Technol. A 6 (3) (1988) 665–670.